Catalysis Communications 11 (2010) 788–791

Contents lists available at ScienceDirect

Catalysis Communications

journal homepage: www.elsevier.com/locate/catcom

Low-temperature catalytic oxidation of toluene over mesoporous MnO_x–CeO_2/TiO_2 prepared by sol–gel method

Danqing Yu, Yue Liu, Zhongbiao Wu *

Department of Environmental Engineering, Zhejiang University, Hangzhou 310027, PR China

ARTICLE INFO

Article history:
Received 1 December 2009
Received in revised form 22 January 2010
Accepted 9 February 2010
Available online 13 February 2010

Keywords:
MnO_x–CeOx/TiO_2 catalyst
Sol–gel method
Catalytic oxidation
Toluene
Ceria modification

ABSTRACT

Sol–gel-made MnO_x/TiO_2 and MnO_x–CeO_2/TiO_2 catalysts were used for low-temperature catalytic oxidation of toluene. The samples were characterized by X-ray diffraction (XRD), nitrogen adsorption–desorption, transmission electron microscope (TEM) and X-ray photoelectron spectroscopy (XPS). The addition of ceria into MnO_x/TiO_2 could greatly improve its activity. Toluene conversion at 180 °C increased dramatically from 57.6% with ceria-free catalyst to 89.4% with the most active ceria-modified catalyst (Ce/Ti = 0.05). The enrichment of well-dispersed amorphous nonstoichiometric manganese oxides and available active oxygen species on the surface of catalysts were considered as main reasons of the enhanced activity after ceria addition.

1. Introduction

Catalytic oxidation can efficiently eliminate dilute volatile organic compounds (VOCs) pollutants at much lower temperatures (300–500 °C) than direct incineration, minimizing the energy consumption [1,2]. The catalysts used can be divided into two major categories: noble metals and transition metal oxides. Noble metal catalysts are generally very active in VOCs deep oxidation [3–5], while transition metal oxides are less expensive and are more resistant to be poisoned by the impurities in the feed stream or the intermediates formed during the oxidation [5–8]. Among the transition metal oxides, manganese oxides (MnO_x) are reported to be efficient in catalytic oxidation, since they contain various types of labile oxygen, which are necessary to complete the catalytic redox cycle [9–11].

Ceria (CeO_2) was potentially advantageous for catalytic applications. Since Ce has two stable oxidation states, Ce^{4+} and Ce^{3+}, oxygen could be stored and released via the redox shift between Ce^{4+} and Ce^{3+}. The ceria doped catalysts exhibit more mobilized active oxygen species, and thus higher activity [1,12,13]. Therefore, ceria-modified MnO_x catalysts would be promising catalysts in catalytic oxidation of VOCs.

Sol–gel method would facilitate the sample to maintain high specific area, controllable pore system and good dispersion of active phase compared to the traditional impregnation method [14,15]. Thus, in this study, the sol–gel method was introduced to prepare MnO_x/TiO_2 and MnO_x–CeO_2/TiO_2 catalysts for low-temperature catalytic oxidation of VOCs. Toluene was chosen as VOC probe molecule, because it is a commonly used solvent and presents an important POCP (Photochemical Ozone Creativity Potential) [16].

2. Experimental

2.1. Catalysts preparation

Tetrabutyl titanate, $Ti(OC_4H_9)_4$, acetic acid, ethanol and water were mixed with the mole ratio of 1:6:10:6 under vigorous stirring at room temperature to form a transparent sol, and the molar ratio of precursor used above was the optimal value obtained in our previous study for sol–gel-made TiO_2 [10]. Certain amount of manganese nitrate (50 wt% solution) and cerium (III) nitrate hexahydrate (used as brought) were added as Mn and Ce sources, respectively, and the Mn/Ti molar ratio was kept as 0.4. After aging for 14 days, the sol transformed to gel. It was dried at 110 °C overnight and calcined at 500 °C for 4 h. The catalyst was denoted as TiMnCe(y), where y represented the Ce/Ti molar ratio, e.g. TiMnCe(0.15).

2.2. Characterizations

The powder XRD patterns were recorded on a Rigaku D/MAX RA diffractometer using Cu Kα radiation at 40 kV and 150 mA. Nitro-

---

* Corresponding author. Address: Department of Environmental Engineering, Yuquan Campus, Zhejiang University, Zheda Road 38, Hangzhou 310027, PR China. Tel.: +86 571 87952459; fax: +86 571 87953088.
E-mail address: zbwu@zju.edu.cn (Z. Wu).

1566-7367/$ - see front matter © 2010 Elsevier B.V. All rights reserved.
doi:10.1016/j.catcom.2010.02.016

gen adsorption–desorption isotherms were obtained on a nitrogen adsorption apparatus (ASAP 2020, USA). Then the specific surface area (S_{BET}) was determined by Brunauer–Emmett–Teller (BET) method, and the pore volume and pore size of the samples were calculated by Barrett–Jioner–Halenda (BJH) method. XPS was performed on a Thermo ESCALAB 250 (USA) apparatus with Al Kα X-rays ($h\nu = 1486.6$ eV) radiation operated at 150 W to investigate the surface atomic concentrations and the oxidation state distribution of the elements in the samples. TEM was used to investigate the microstructures, morphologies and grain size of the prepared samples with a JOEL JEM-2010 (Japan) electron microscope.

2.3. Catalytic activity test

The activities of the catalysts were measured in a fixed bed reactor. The 6-mm i.d. quartz reactor tube, loaded with 0.6 ml catalyst powder, was located in an electrically heated furnace. The flow rate was set to maintain the gas hourly space velocity (GHSV) at 15,000 h^{-1} for all the runs. A nitrogen stream bubbling through a saturator filled with liquid toluene in an ice-water bath, and it was then mixed with 6% O_2/N_2 gas stream, to keep the inlet concentration at about 1000 ppm. The catalyst bed was firstly preheated to 320 °C for 2 h under the reactant mixture to avoid the fluctuations in activity observed when the reaction was carried out with fresh catalysts. The temperature was then changed from 240 to 80 °C in steps of 20–40 °C, and conversion were measured typically 30–50 min after a desired temperature was arrived at. The reactants and products were analyzed using a Fuli 9790 gas chromatograph (GC) equipped with a flame ionization detector (FID). No other carbon-containing organic compounds were detected.

3. Results and discussion

3.1. Catalytic performance for oxidation of toluene

According to the previous results (not shown here), when Mn/Ti equal to 0.4, the catalyst was the most active catalyst among the MnO_x/TiO_2 catalysts, and it could oxidize toluene completely at 240 °C. Its T_{50} and T_{90} (temperature at which 50% and 90% conversion is achieved, respectively) values for toluene combustion were 175 and 197 °C, similar with or even lower than the results reported by other authors [17–20] under comparable operating conditions. To improve the activity further, ceria was added into this catalyst, and the corresponding toluene light-off curves are shown in Fig. 1.

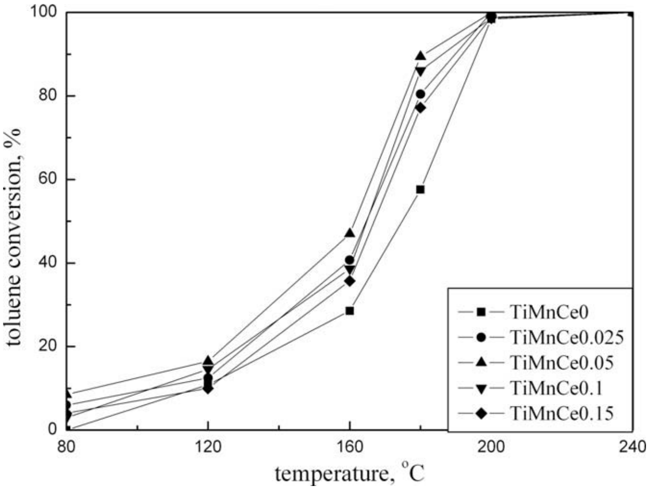

Fig. 1. Light-off curves of toluene over MnO_x/TiO_2 and MnO_x–CeO_2/TiO_2 catalysts. Reaction conditions: 1000 ppm toluene, 6% oxygen, and balance N_2, GHSV = 15,000 h^{-1}.

After ceria was added, the activities of the catalysts were improved, especially in high temperatures range. There was an optimal content of ceria added. It was found that TiMnCe(0.05) showed a superior activity than the other ceria-modified catalysts. Toluene conversion at 180 °C increased dramatically from 57.6% with TiMnCe(0) catalyst to 89.4% when TiMnCe(0.05) was employed. And the temperature for completed conversion of toluene was 40 °C lower than that for ceria-free catalyst. Taking the high activity of TiMnCe(0) catalyst into account, this activity enhancement could not be negligible.

3.2. Textural properties of catalysts

The XRD patterns of the catalysts are shown in Fig. 2. A strong peak at $2\theta = 25.5°$ of anatase TiO_2 was detected in all XRD diagrams. There was a poorly resolved peak at $2\theta = 37°$ for TiMnCe(0) ascribing to the pyrolusite MnO_2 phase [21,22]. However, no signals of MnO_x species appeared after ceria addition, indicating that ceria could modify the dispersion of supported active phases even at very loading content. Although no evident diffraction peaks of ceria species were observed, a broad and flat peak spanning over 30–40° emerged when Ce/Ti exceeded 0.05, and this peak become more evident with the increment of ceria content. Therefore it might be attributed to partial crystallization of fluorite ceria [21,22]. The introduced ceria might also interact with the titania support, tampering its crystallization, since the intensity of the anatase signal decreased dramatically after the addition of ceria.

Fig. 3 shows the TEM images of some selected catalysts. Calculated from the Fig. 3a and b, the mean particle size of the TiMnCe(0) and TiMnCe(0.05) are 11.4 and 10.8 nm, respectively, consistent with the XRD results. The well-crystallized anatase titania could be seen in both catalysts (whose lattice fringe is 0.354 nm), while no crystalline structure of CeO_2 could be seen in the high-resolution transmission electron microscopy (HRTEM) (Fig. 3c and d). In accordance with the XRD results, MnO_2 crystalline can be found in the ceria-free sample (the inset in Fig. 3c) (whose lattice fringe is 0.237 nm, conforming to the ICDD-JCPDS database), while it is absent in the TiMnCe(0.05) samples. Because of the interaction of ceria with titania and manganese oxides as mentioned above, the smaller particle size and improved MnO_x active phase dispersion were observed.

The textural parameters of the samples, such as BET specific surface area (S_{BET}), pore volume (V_p), and average pore radius (r_p)

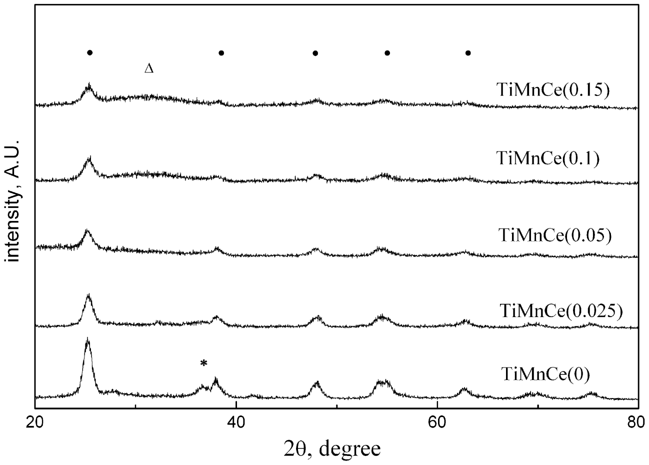

Fig. 2. XRD patterns of the MnO_x/TiO_2 and MnO_x–CeO_2/TiO_2 catalysts. ● Anatase TiO_2, Δ cerium oxide Ce_2O_3, * pyrolusite MnO_2.